Electronic Supporting Information

Catechol-TiO_2 hybrids for photocatalytic H_2 production and photocathode assembly

Katherine L. Orchard, Daisuke Hojo, Katarzyna P. Sokol, Meng-Ju Chan, Naoki Asao, Tadafumi Adschiri, Erwin Reisner

1. Experimental Details

1.1 Materials

Reagents. Aeroxide® TiO_2 P25 nanoparticles; anatase/rutile (8:2) mixture, average diameter: 21 nm) were provided by Evonik Industries. Anatase nanoparticles (10 nm average diameter, AN10-TiO_2) were provided by MKnano, Canada (product MKN-TiO2-C7). Na_2SO_4 (99 %) was purchased from Alfa Aesar. Indium tin oxide nanoparticles (< 50 nm), 3,4-dihydroxyhydrocinnamic acid (DHCA, 98 %), caffeic acid (CA, ≥ 98 %) and triethyloxonium tetrafluoroborate (1.0 M in dichloromethane) were purchased from Sigma-Aldrich. Ammonium hydroxide (30 wt%), hydrogen peroxide (30 %), and triethylamine (TEA) were purchased from Fisher Scientific. $[Ni(P^{Ph}{}_2N^{C_6H_4CH_2P(O)(OH)_2}{}_2)_2]Br_2 \cdot HBr$, **NiP**, was prepared according to a literature procedure.[1] Diethyl (*E*)-2-(3,4-dihydroxyphenyl)vinylphosphonate was synthesised according to a literature procedure.[2] Ultra-pure water (18.2 MΩ·cm, Milli-Q®) was used for all aqueous solutions.

Electrode materials. Tin-doped indium oxide coated glass (ITO, 12 Ω sq^{-1}) was purchased from VisionTek Systems Ltd. Fluorine-doped tin oxide coated glass (FTO, 7 Ω sq^{-1}) was purchased from Sigma-Aldrich. Mesoporous ITO (*meso*ITO) was deposited onto ITO by the doctor-blading technique, following a previously reported method.[3] Hierarchical inverse-opal ITO was deposited onto FTO by a previously reported colloidal co-assembly method.[4, 5]

1.2 Physical Measurements

The pH of aqueous solutions was measured using a Mettler Toledo S20 SevenEasy™ pH meter, and adjustments to pH were made using dilute solutions of NaOH and H_2SO_4. Transmission Electron Microscopy (TEM) images were collected using a FEI Philips Tecnai 20 instrument, with 200 kV accelerating voltage; samples were drop-cast onto holey carbon films (TAAB Laboratories Equipment Ltd). Scanning Electron Microscopy (SEM) was carried out using a FEI Philips XL30 sFEG instrument and energy dispersive X-ray analysis (EDX) was carried out using an X-Max SDD Detector (Oxford Instruments). High resolution SEM images of the nanoparticles were obtained using an FESEM (JSM-7800F, JEOL) at an acceleration voltage of 15 KV. Inductively Coupled Plasma-Optical Emission Spectroscopy (ICP-OES) was carried out by Mr Alan Dickerson (Department of Chemistry, Cambridge). Samples for TiO_2 analysis were digested in 2:1 H_2SO_4:HNO_3 at 210 °C for 45 min using a microwave synthesiser (Biotage® Initiator+);[6] samples for Pt analysis were digested in aqua regia at 80 °C for 30 min. Ultraviolet-Visible (UV-Vis) spectroscopy was carried out using a Varian Cary 50 UV-Vis spectrophotometer. Fourier-transform infrared (FT-IR) spectra were obtained using a Thermo Scientific Nicolet iS50 FTIR spectrometer in attenuated total reflection (ATR) mode. ^{1}H NMR spectra were recorded on JEOL JMTC-270/54/SS (JASTEC, 400 MHz) and BRUKER (600 MHz) spectrometers. High-resolution mass spectra (HRMS) were obtained on a BRUKER APEXIII spectrometer.

1.3 Synthetic Procedures

1.3.1 Organic molecules:

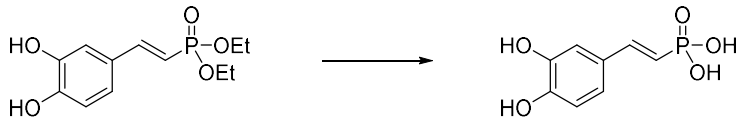

(*E*)-(3,4-dihydroxystyryl)phosphonic acid (DHSP). To a solution of diethyl (*E*)-2-(3,4-dihydroxyphenyl)vinylphosphonate (200 mg, 0.73 mmol) in CH_2Cl_2 (2 mL) was added TMSBr (389 µl, 2.92 mmol) at 0 °C, and the mixture was stirred at room temperature for 3 h. Excess TMSBr and solvents were evaporated under reduced pressure. The residue was dissolved with CH_2Cl_2 (2 mL), and the solvents were evaporated again for complete removal of the remaining TMSBr. To the resulting materials were added CH_2Cl_2 (2 mL) and D_2O (2 mL) at 0 °C, and the mixture was stirred at room temperature overnight. Then, volatile organic materials were evaporated under diminished pressure to afford the target molecule as a D_2O solution. The chemical yield was determined to be 78 % by NMR using MeOH as an internal standard; due to the instability of this molecule at room temperature, it was stored as an aqueous solution at 4 – 8 °C. ^{1}H NMR (700 MHz, D_2O): δ = 6.11 (dd, $^3J_{HH}$ = 17.5 Hz, $^2J_{HP}$ = 18.9 Hz, 1 H, CHP), 6.73 (d, $^3J_{HH}$ = 8.4 Hz, 1 H, CH_{Ar}), 6.85 (dd, $^3J_{HH}$ = 8.4 Hz, $^4J_{HH}$ = 2.1 Hz, 1 H, CH_{Ar}), 6.93 (d, $^4J_{HH}$ = 2.1 Hz, 1 H, CH_{Ar}), 7.07 (dd, $^3J_{HP}$ = 23.1 Hz, $^3J_{HH}$ = 17.5 Hz, 1 H, CHAr). ^{13}C NMR (176 MHz, D_2O): d = 113.12 (d, $^1J_{CP}$ = 186.7 Hz, PCH), 114.67 (CH_{Ar}), 116.25 (CH_{Ar}), 121.69 (CH_{Ar}), 128.10 (d, $^3J_{CP}$ = 24.3 Hz, C_{Ar}), 144.29 (C_{Ar}), 146.30 (d, $^2J_{CP}$ = 6.2 Hz, CHAr), 146.39 (C_{Ar}). HRMS (ESI, negative ion mode): m/z calcd. for $C_8H_8O_5P$ 215.0109, found 215.0115 $[M - H]^-$.

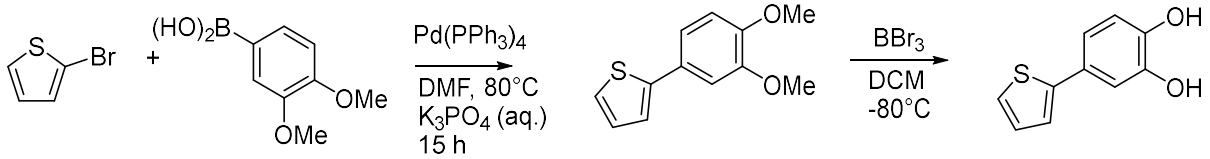

Synthesis of 2-(3,4-dihydroxybenzene)thiophene, DHBT.[7] Under N_2, a solution of K_3PO_4 (0.423 g, 1.99 mmol) in water (3 mL) was added to a solution of 2-bromothiophene (87 µL, 0.902 mmol), 3,4-dimethoxyphenylboronic acid (0.324 g, 1.80 mmol), and tetrakis(triphenylphosphine)palladium(0) (104 mg, 0.09 mmol) in dry dimethylformamide (15 mL). The mixture was placed in an oil bath at 90 °C for 16 h. The reaction solution was quenched with water (100 mL) and extracted with ethyl acetate (300 mL). The organic phase was washed with water (50 mL) and brine (50 mL), dried over magnesium sulphate, and the solvent evaporated to dryness. The product was purified by column chromatography (silica gel, 8 % ethyl acetate/hexane) to give the intermediate 2-(dimethoxybenzene)thiophene as a white powder (153 mg, 77 %). ^{1}H NMR (400 MHz, $CDCl_3$) δ = 7.25 (1H, *dd*, J_1 = 1.2 Hz, J_2 = 5.1 Hz), 7.26 (1H, *dd*, J_1 = 1.2 Hz, J_2 = 3.6 Hz), 7.20 (1H, *dd*, J_1 = 8.3 Hz, J_2 = 2.2 Hz), 7.14 (1H, *d*, *J* = 2.1 Hz) , 7.09 (1H, *dd*, J_1 = 3.6 Hz, J_2 = 5.1 Hz), 6.86 (1H, *d*, *J* = 8.3 Hz), 3.92 (3H, *s*), 3.89 (3H, *s*) ppm.

Under N_2, boron tribromide (1.0 M in dichloromethane, 1.5 mL) was added dropwise to a solution of 2-(dimethoxybenzene)thiophene (50 mg, 0.255 mmol) in dichloromethane (1.5 mL) at –78 °C. The solution was stirred at this temperature for 3 h then allowed to warm to room temperature for a further 3.5 h before quenching with water (2 mL) at 0 °C. The reaction mixture was extracted with ethyl acetate (10 mL), washed with brine (10 mL), dried over magnesium sulphate, and the solvent

evaporated to dryness. The residue was purified by column chromatography (silica gel, 40 % ethyl acetate/hexane) to give **1** as a white powder (23 mg, 47 %). ^{1}H NMR (CD_3OD) δ = 7.24 (1H, *dd*, J_1 = 1.1 Hz, J_2 = 5.1 Hz), 7.17 (1H, *dd*, J_1 = 1.2 Hz, J_2 = 3.6 Hz), 7.06 (1H, *d*, *J* = 2.4 Hz), 7.02 (1 H), 6.96 (1H, *dd*, J_1 = 8.2 Hz, J_2 = 2.2 Hz), 6.77 (1H, *d*, *J* = 8.2 Hz) ppm. MS (ESI, negative ion mode) *m/z* calcd. for $C_{10}H_7O_2S$ 192.02, found 191 $[M - H]^-$.

1.3.2 Nanoparticle powders:

Anatase nanoparticles, AN7-TiO_2. Oleic acid-capped TiO_2 (6.8 ± 0.7 nm; OA-AN7-TiO_2) were synthesised by a previously reported method.[8] Briefly, titanium tetraisopropoxide (1 mmol), oleic acid (3 mmol) and hexadecylamine (0.5 mmol) were mixed and heated to 120 °C for 5 min. The mixture was transferred to a pressure-resistant Hastelloy vessel (inner volume = 5 mL) and heated at 400 °C for 10 min. The particles were isolated with cyclohexane (3 mL) and washed with ethanol (3 mL). After three washing cycles, the particles were finally suspended in cyclohexane (5 mL).

Catechol-functionalised commercial TiO_2. Based on a literature procedure,[9] P25 and MKN were functionalised using an excess of catechol (10:1 TiO_2:catechol by weight). For example: TiO_2 (200 mg) was suspended in acetone (200 mL) and sonicated for 10 min to ensure good dispersion. 3,4-dihydroxyhydrocinnamic acid (DHCA, 20 mg) was added and the mixture stirred for a further 5 min. A yellow/orange colour was formed immediately on adding DHCA. The solvent was reduced to approximately 40 mL on a rotary evaporator and the particles were isolated by centrifugation (4000 rpm, 5 min). The particles were washed with acetone (50 mL), centrifuged (4000 rpm, 5 min) and allowed to dry in air. Functionalisation was carried out on the same scale and in acetone for all derivatives except for DHBT, which was carried out in methanol on a 30 mg scale.

Caffeic acid functionalised anatase TiO_2 (CA-AN7-TiO_2). Oleic acid ligands were removed from AN7-TiO_2 using a modified ligand-stripping procedure.[10] Under inert atmosphere, anhydrous acetonitrile (1 mL) was placed into a Schlenk flask and AN7-TiO_2 in cyclohexane (1 mL, 0.5 wt%) was layered on top. Triethyloxonium tetrafluoroborate solution (2 × 50 µL) was added and the solution vigorously stirred. Anhydrous hexane (2 mL) was added, followed by triethyloxonium tetrafluoroborate solution (50 µL). The particles were isolated by adding anhydrous $CHCl_3$ (3 mL) and centrifuging (7000 rpm, 3 min). After drying for 1 min, the particle pellet was redispersed in DMF (200 µL). The TiO_2 content was determined by calcining a known quantity of dried solution at 500 °C in a furnace and measuring the mass difference. CA-AN7-TiO_2 was prepared by adding an excess of caffeic acid (1 mM in DMF) to a solution of stripped TiO_2 (50 mg mL^{-1} in DMF). The solution was stirred in the dark for several hours before isolating with excess $CHCl_3$ and collecting the particles by centrifugation. The particles were redispersed in methanol (50 mg mL^{-1}).

1.3.3 Photoelectrode preparation:

Functionalisation with CA-P25 powder. A solution of CA-P25 (5 wt% in ethanol) was spin-coated onto electrodes at 2000 rpm (10 s).

Functionalisation with DHSP. Electrodes were placed in a mixture of water, NH_4OH (30 %) and H_2O_2 (30 %) in a ratio of 5:1:1, heated to 70 °C for 30 min and then rinsed with water and dried for 30 min at 150 °C. They were then placed in a solution of (*E*)-(3,4-dihydroxystyryl)phosphonic acid (DHSP, 1 mM in water) at 4 – 8 °C for 16 h. The electrodes were rinsed with water and allowed to dry at room temperature. Electrodes functionalised with DHSP alone were not stable beyond 1-2

weeks, as evidenced by loss of the redox couple in cyclic voltammetry; therefore, these electrodes were typically used within 1 day of preparation.

Deposition of AN7-TiO_2. Electrodes were immersed face down in a solution of OA-AN7-TiO_2 (100 µL, 0.05 wt% in toluene) for 16 h, rinsed with toluene and dried in air in the dark. OA ligands were removed by soaking in 10 % TEA in ethanol for 2 h. ITO|DHSP|TiO_2 electrodes prepared in this way were stable on storage; however, these electrodes were typically tested within 1-2 weeks of preparation.

Deposition of P25 TiO_2. A suspension of P25 (5 wt% in ethanol) was either spin-coated onto electrodes at 2000 rpm (10 s; for data shown in Fig. S12) or deposited by immersion of the electrode in the suspension for 16 h (for data shown in Fig. S16). The deposition procedure did not affect the final photocurrent measured.

Deposition of NiP. ITO|DHSP|AN7-TiO_2 electrodes were immersed in aqueous **NiP** solutions (200 µL) of a range of concentrations (0.01 – 1 mM) and pH values (~2 – 4.5), with immersion times from 1 – 16 h. After immersion, the electrodes were rinsed with H_2O and allowed to air dry before testing. Electrodes were tested within 1 day of preparation.

1.4 Photocatalysis

All solution photocatalysis experiments were carried out using a Solar Light Simulator (Newport Oriel, 1000 W, 100 mW cm^{-2}) fitted with an air mass 1.5 global filter (AM1.5G). IR and UV irradiation were removed using a water filter and a 420 nm cut-off filter, respectively. Reaction solutions were maintained at 25 °C throughout irradiation by a temperature-controlled water bath. Ascorbic acid (AA) solutions (0.1 M, pH 4.5) and **NiP** stock solutions (1 mM in methanol) were always prepared freshly before use. A total solution volume of 2.25 mL was used, and experiments were carried out in Pyrex-glass reaction vessels with a calculated final headspace volume of 2.33 mL.

Method In a typical procedure, TiO_2 powder (2.5 mg) was suspended in the AA buffer solution (2.2 mL) with sonication for 10 min. The catalyst stock solution (50 µL, 0.05 µmol) was added under stirring. The reaction vessel was protected from light with aluminium foil and purged with 2 % CH_4 in N_2 for at least 10 min before beginning the light experiment. Aliquots of the headspace gas (20 µL) were taken at regular intervals and analysed using an Agilent 7890 series gas chromatograph; CH_4 was used as an internal standard to calculate the volume of H_2 evolved.

External quantum efficiency (EQE)

Photocatalysis solutions (2.25 mL total volume, 5 mg CA-P25, 0.05 µmol **NiP**, 0.1 M AA, pH 4.5) were prepared in a quartz, flat-sided cuvette (1 cm pathlength) and purged with 2 % CH_4 in N_2. They were then irradiated using a LOT Quantum Design MSH-300 monochromator. Aliquots of headspace gas were analysed after 3 h.

The EQE was calculated according to:

$$EQE\ (\%) = \frac{2(nH_2)N_A hc}{t_{irr}\lambda EeA} \times 100$$

where N_A is the Avogadro constant, h is the Planck constant, c is the speed of light, t_{irr} is the irradiation time, A is the irradiated area (0.25 cm^2), λ is the irradiation wavelength (420 ± 5 nm) and Ee is the irradiance (1.5 mW cm^{-2}).

1.5 (Photo)electrochemical Procedures

In general, all (photo)electrochemical measurements were carried out in a three-electrode setup, with a Ag/AgCl (sat. KCl) reference and Pt mesh counter electrode. A PalmSens EmStat potentiostat or an Ivium Technologies CompactStat was used. Aqueous (photo)electrochemistry was carried out in a custom-made, two-compartment cell, with the working and reference electrodes separated from the counter by a Nafion® proton exchange membrane. Na_2SO_4 (0.1 M) was used as the electrolyte, and the pH adjusted with dilute solutions of HCl or NaOH. Unless otherwise stated, solutions were irradiated with a 250 W Quartzline® projection lamp fitted with a 400 nm cut-off filter (ThorLabs, Inc.) and an intensity at the electrode surface of 100 mW cm^{-2}. For simulated solar irradiation, a solar light simulator (Newport Oriel) equipped with an air mass 1.5 global filter was used. Changing the cut-off filter to >420 nm yielded photocurrents of similar magnitude to those obtained with the >400 nm filter.

Calculation of loading of DHSP

The area under the oxidation peak (forward scan) in the cyclic voltammogram (CV) of DHSP immobilised on IO-ITO was integrated in order to calculate the total charge passed (in C). The charge was divided by the Faraday constant (9.649×10^4 C mol^{-1}) to give the number of moles of electrons passed. The number of molecules of DHSP per electrode was estimated assuming that 2 electrons are required to fully oxidise each molecule of DHSP, and the loading of DHSP per cm^2 was obtained by multiplying the DHSP per electrode by 4.

1.6 Attachment studies

Competition between catechol and phosphonic acid groups

Binding of catechol groups to TiO_2 or ITO surfaces in the presence or absence of phosophonic acid groups was carried out by recording the UV-vis absorption spectrum of a DHCA solution before and after exposure to the respective particles.

ITO: IO-ITO electrodes were immersed in an aqueous solution of DHCA (0.5 mM, 200 µL) with or without 1 equivalent of propylphosphonic acid. After 16 h, the electrodes were removed and an aliquot of the catechol solution (100 µL) was diluted with water (1 mL) and the UV-vis spectrum recorded.

TiO_2: P25 powder (2.5 mg) was suspended in H_2O (2 mL) with sonication. A stock solution of either DHCA or 1:1 DHCA:propylphosphonic acid (200 µL, 1 mM each in H_2O) was added and the suspension stirred for 1 h in the dark. The powders were isolated by centrifugation (7000 rpm, 5 min) and the supernatant was filtered (200 µm filter) before analysis.

Attachment of NiP to CA-TiO_2

CA-TiO_2 powders (1 mg) were suspended in AA solution (0.9 mL, 0.1 M, pH 4.5) with sonication. A stock solution of **NiP** (100 µL, 1 mM) was added and the solutions stirred in the dark for 1 h. The powders were isolated by centrifugation (7000 rpm, 5 min) and the supernatant was filtered (200 µm filter). Aliquots of the filtered solution (100 µL) were diluted with fresh AA solution (1 mL) before analysis.

2. Supplementary Tables

Table S1. Estimates of dye loading on TiO_2 nanoparticles from measured carbon content (elemental analysis). Catechol = 1,2-dihydroxybenzene, DHBA = 3,4-dihydroxybenzoic acid, DHCA = 3,4-dihydroxyhydrocinnamic acid, CA = caffeic acid, DHBT = 2-(3,4-dihydroxybenzene)thiophene, ND = 2,3-naphthalenediol, AA = ascorbic acid.

Dye	TiO_2	C / %	C / µg (mg powder)$^{-1}$	Dye / nmol (mg powder)$^{-1}$
Catechol	P25	0.7[a]	7.2	99.9
DHBA	P25	1.1[a]	11.2	133.2
DHCA	P25	1.8[b]	18.5	171.5
CA	P25	1.3[a]	12.6	116.6
DHBT	P25	0.9[a]	9.0	74.9
ND	P25	1.3[a]	12.6	104.9
AA	P25	1.2[a]	12.3	170.7
CA	MKN	5.5[a]	54.6	505.1

[a] Single measurement

[b] Average of measurements from 3 independent batches of DHCA-P25 powder. Standard deviation in %C = ± 0.1.

Table S2. Comparison of photocatalytic H_2 evolution from charge-transfer dye-functionalised TiO_2. Conditions: 0.1 M AA, pH 4.5, 2.5 mL, λ > 420 nm, AM 1.5 G, 100 mW cm^{-2}, 25 °C.

Dye	TiO_2	Powder / mg	NiP / µmol	Time / h	H_2 / µmol	Activity / µmol H_2 g^{-1}	TON / Ni^{-1}	TON† / dye^{-1}
Dye variation								
No dye	P25	2.5	0.05	1	0.042 ± 0.004	16.8 ± 1.7	0.84 ± 0.08	-
				4	0.16 ± 0.03	63.8 ± 13.7	3.19 ± 0.69	-
Catechol	P25	2.5	0.05	1	0.10 ± 0.03	41.8 ± 9.9	2.09 ± 0.49	0.42 ± 0.10
				4	0.33 ± 0.05	133.6 ± 19.1	6.68 ± 0.95	1.34 ± 0.19
DHBA	P25	2.5	0.05	1	0.11 ± 0.01	43.5 ± 2.3	2.18 ± 0.11	0.33 ± 0.02
				4	0.41 ± 0.02	164.3 ± 9.1	8.21 ± 0.46	1.23 ± 0.07
DHCA	P25	2.5	0.05	1	0.11 ± 0.01	44.9 ± 3.0	2.25 ± 0.15	0.29 ± 0.02
				4	0.44 ± 0.02	175.1 ± 5.8	8.76 ± 0.29	1.11 ± 0.04
CA	P25	2.5	0.05	1	0.19 ± 0.01	77.0 ± 3.4	3.85 ± 0.17	0.66 ± 0.03
				4	0.68 ± 0.07	272.8 ± 28.6	13.64 ± 1.43	2.34 ± 0.25
DHBT	P25	2.5	0.05	1	0.12 ± 0.04	46.8 ± 13.9	2.34 ± 0.70	0.63 ± 0.19
				4	0.43 ± 0.11	171.5 ± 43.7	8.58 ± 2.18	2.29 ± 0.58
ND	P25	2.5	0.05	1	0.07 ± 0.02	28.6 ± 5.8	1.43 ± 0.29	0.27 ± 0.06
				4	0.29 ± 0.03	117.2 ± 10.8	5.86 ± 0.54	1.12 ± 0.10
AA	P25	2.5	0.05	1	0.06 ± 0.01	23.4 ± 4.2	1.17 ± 0.21	0.13 ± 0.02
				4	0.28 ± 0.03	111.6 ± 1.1	5.58 ± 0.06	0.63 ± 0.01
Particle variation								
CA	AN10	2.5	0.05	3	0.33 ± 0.04	130.4 ± 15.1	6.52 ± 0.75	0.26 ± 0.02
CA	AN7	2.5	0.05	3	0.03 ± 0.003	9.8 ± 1.3	0.49 ± 0.07	-
CA	R	2.5	0.05	3	0.012 ± 0.001	4.9 ± 0.3	0.24 ± 0.01	-
NiP variation								
CA	P25	2.5	0.010	3	0.28 ± 0.06	110.7 ± 25.3	27.7 ± 6.3	0.95 ± 0.21
		2.5	0.025	3	0.42 ± 0.07	166.3 ± 26.7	16.6 ± 2.7	1.43 ± 0.23
		2.5	0.050	3	0.55 ± 0.09	220.1 ± 36.6	11.0 ± 1.8	1.88 ± 0.31
Powder loading								
CA	P25	0.6	0.05	3	0.04 ± 0.01	67.9 ± 11.9	0.81 ± 0.14	0.58 ± 0.10
		1.25	0.05	3	0.28 ± 0.07	221.0 ± 59.9	5.5 ± 1.5	1.90 ± 0.51
		5.0	0.05	3	1.04 ± 0.09	207.2 ± 18.1	20.7 ± 1.8	1.78 ± 0.15
Light intensity								
100% transmission								
CA	P25	2.5	0.05	3	0.55 ± 0.09	220.1 ± 36.6	11.0 ± 1.8	1.83 ± 0.30
50% transmission								
CA	P25	2.5	0.05	3	0.43 ± 0.05	171.0 ± 21.3	8.5 ± 1.1	1.47 ± 0.18
20% transmission								
CA	P25	2.5	0.05	3	0.13 ± 0.02	52.4 ± 10.0	2.6 ± 0.5	0.45 ± 0.09

† TON per dye reported as µmol H_2 per µmol dye; however, note that the actual TON is twice that reported as two photoelectrons must be generated per molecule of H_2.

Table S3. Comparison of photocurrents in the presence of air for charge-transfer dye-functionalised TiO_2 photoelectrodes (0.3 V vs RHE, 0.1 M Na_2SO_4, pH 4.5, λ > 400 nm, room temperature).

Type	ITO	Catechol	TiO_2	| *j* | / μA cm^{-2}
Pre-functionalised	meso	none	CA-P25	2.5 ± 0.75
Layer-by-layer	meso	DHSP	P25	2.9 ± 0.2
Layer-by-layer	meso	DHSP	AN10	2.9 ± 0.2
Layer-by-layer	meso	DHSP	AN7	18.4 ± 4.6
Layer-by-layer	IO-2 μm	DHSP	AN7	14.5 ± 4.0
Layer-by-layer	IO-4 μm	DHSP	AN7	49.6 ± 8.5[a]
Layer-by-layer	IO-12 μm	DHSP	AN7	69.0 ± 4.8

[a]Single measurement; the error given is the expected error based on the average error of all electrode measurements (17.2%)

3. Supplementary Figures

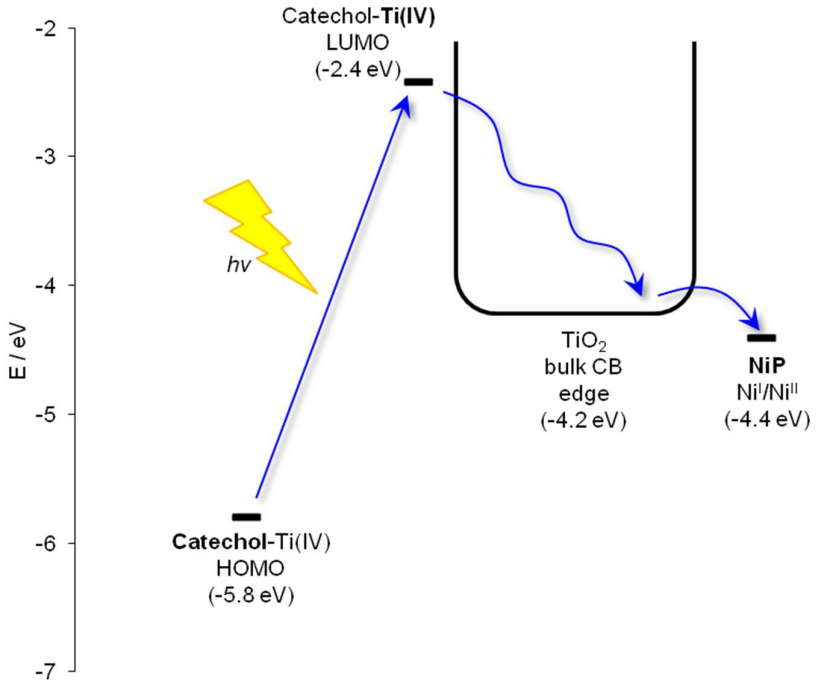

Figure S1. Energy level diagram of the catechol-TiO_2-**NiP** photocatalytic H_2 evolution system. Excitation occurs by LMCT from catechol to a surface Ti^{4+} centre, followed by rapid delocalisation into the TiO_2 conduction band (CB) and reduction of the H_2 evolution catalyst, **NiP**. Catechol-Ti(IV) HOMO/LUMO levels are taken from Ooyama et al.,[11] the TiO_2 bulk conduction band is taken from Xu et al,[12] and the **NiP** redox potential is taken from Gross et al..[1]

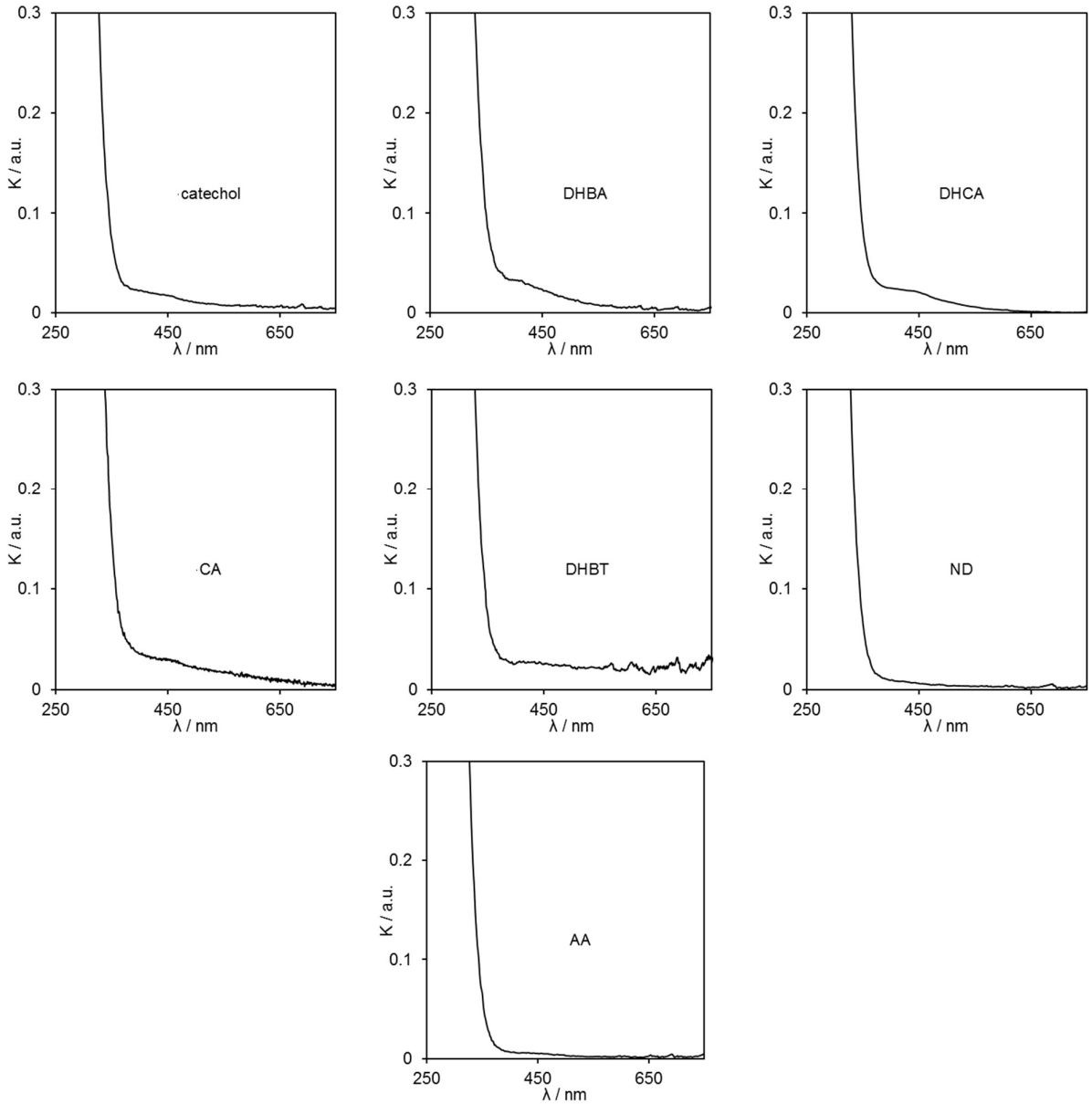

Figure S2. Diffuse reflectance UV-vis spectra of charge-transfer dye-functionalised P25 TiO_2 (1 wt% in Ba_2SO_4). Top to bottom (left to right): 1,2-dihydroxybenzene (catechol), 3,4-dihydroxybenzoic acid (DHBA), 3,4-dihydroxyhydrocinnamic acid (DHCA), caffeic acid, 2-(3,4-dihydroxybenzene)thiophene (DHBT), 2,3-naphthalenediol (ND), and ascorbic acid (AA). Spectra are normalised to the absorption at 300 nm.

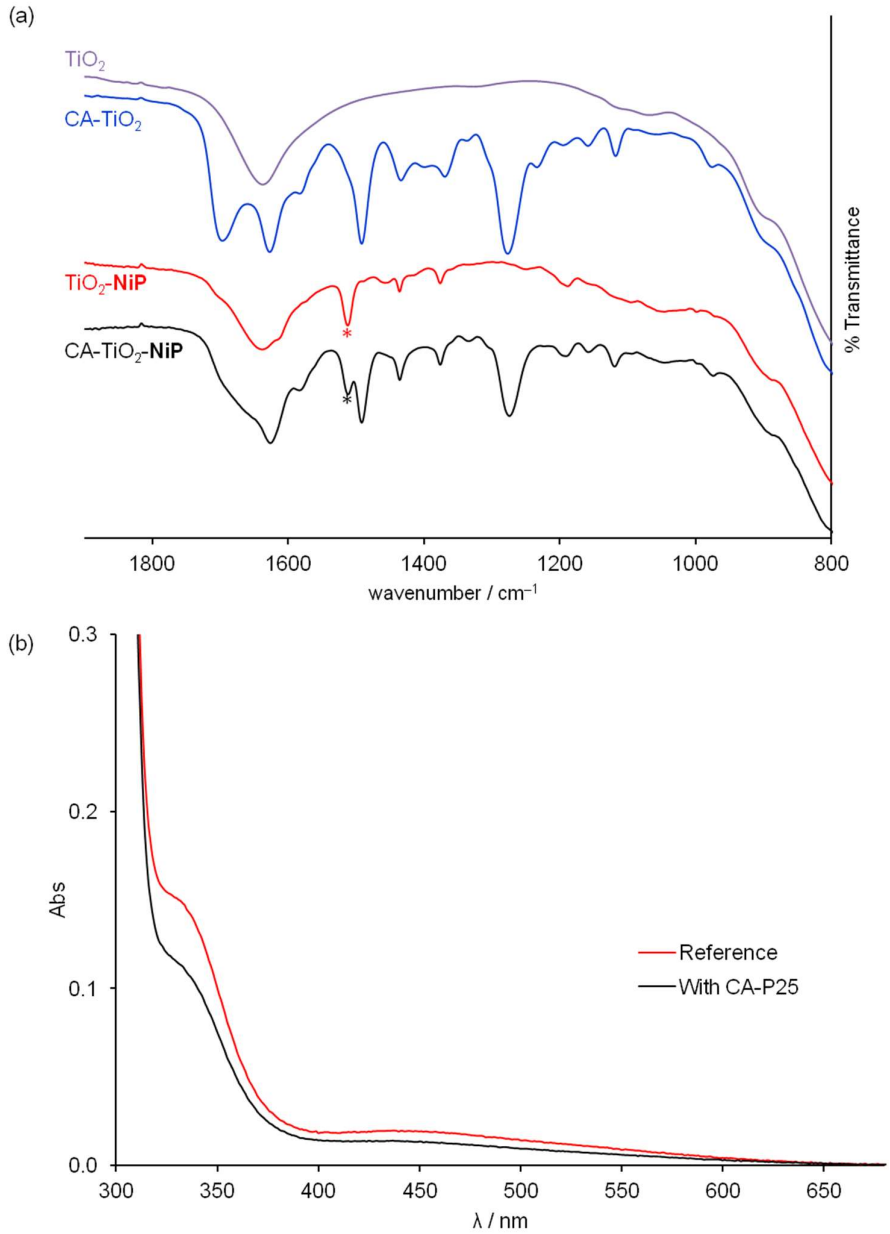

Figure S3. (a) FTIR spectroscopy of TiO_2 nanoparticles (AN10-TiO_2) functionalised with CA and **NiP**, with characteristic peaks of both **NiP** and CA present in the hybrid particle spectrum (CA-TiO_2-**NiP**); (b) UV-vis spectroscopy of an aqueous **NiP** solution (0.1 M AA, pH 4.5) before (Reference curve, red) and after (black curve) exposure to CA-P25.

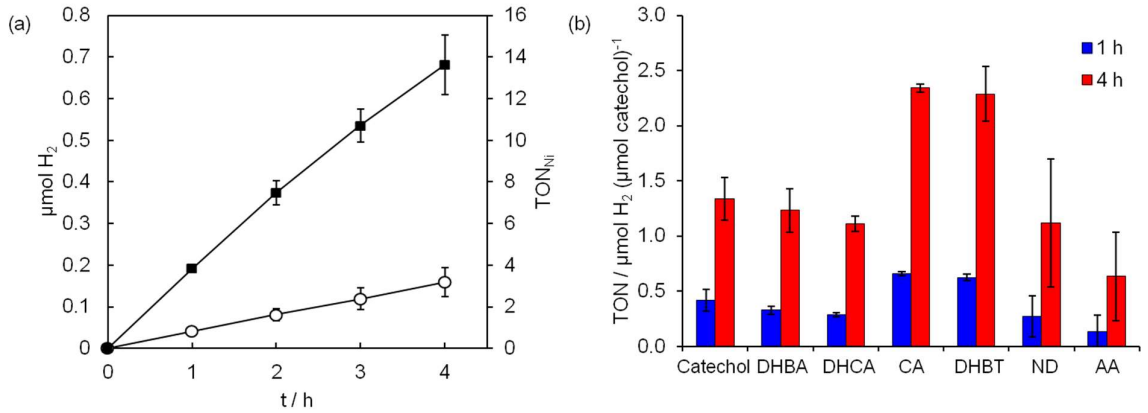

Figure S4. Comparison of visible-light driven H_2 evolution with charge-transfer dye-functionalised P25 TiO_2 powders in the presence of a molecular Ni catalyst, **NiP** (a) H_2 evolution from CA-P25 (black squares) and bare P25 (white circles) over time, and (b) correlation of activity with catechol loading. Catechol loading was estimated by elemental analysis (carbon content; Table S1). Conditions: 0.1 M AA, pH 4.5, 2.5 mg powder, 50 nmol **NiP**, 2.25 mL, λ > 420 nm, AM 1.5 G 100 mW cm^{-2}, 25 °C.

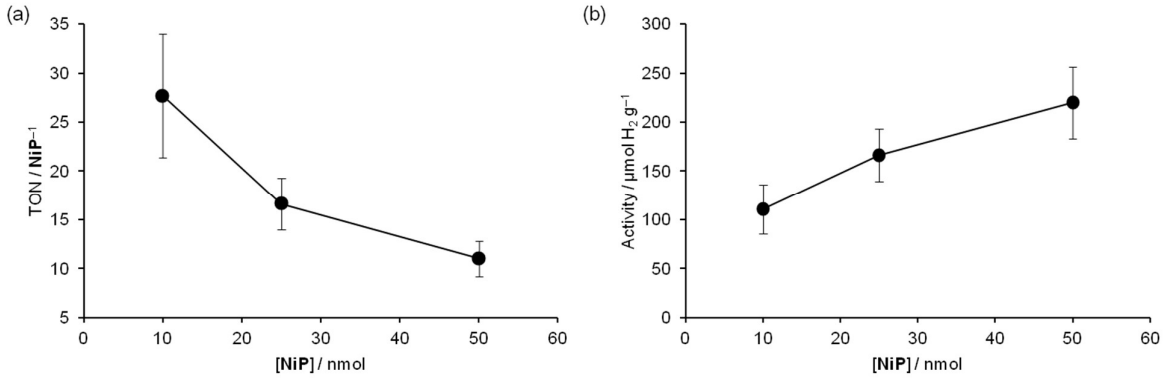

Figure S5. Effect of catalyst loading on (a) turnover per catalyst and (b) activity per g powder for CA-P25 sensitised DSP. Conditions: 2.5 mg CA-P25, 2.25 mL electron donor solution (0.1 M AA, pH 4.5), AM 1.5 G 100 mW cm^{-2}, λ > 420 nm, 25 °C.

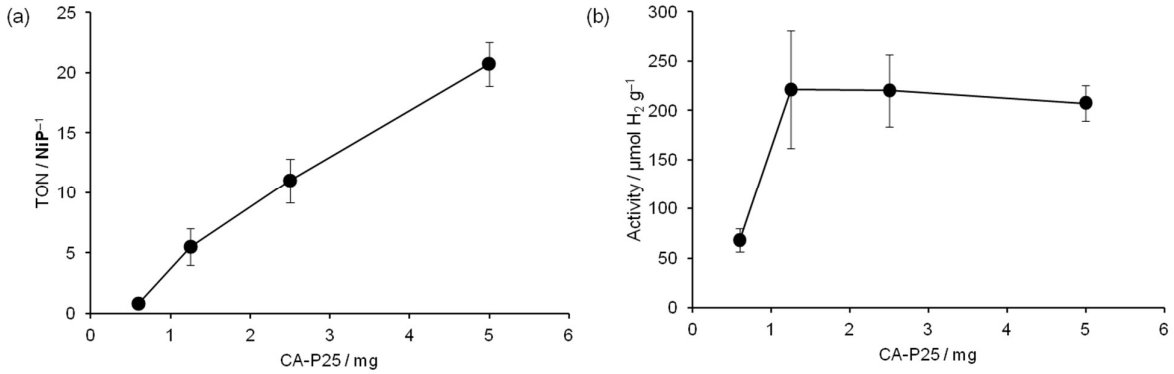

Figure S6. Effect of powder loading on (a) turnover per catalyst and (b) activity per g powder for CA-P25 sensitised DSP. Conditions: 0.05 μmol **NiP**, 2.25 mL electron donor solution (0.1 M AA, pH 4.5), AM 1.5 G, 100 mW cm^{-2}, λ > 420 nm, 25 °C.

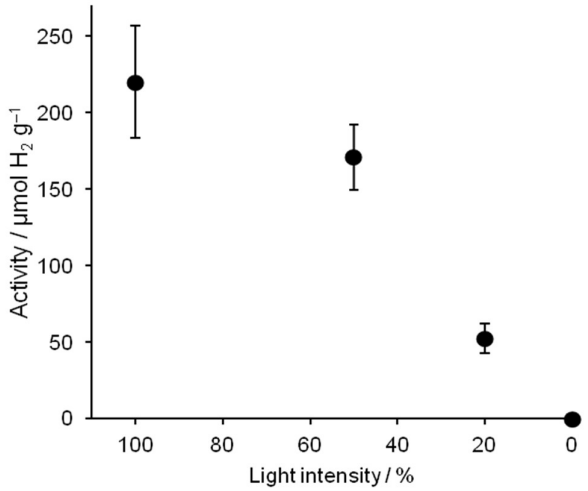

Figure S7. Effect of light intensity on activity per g powder for CA-P25 powders, measured using neutral density filters. Conditions: 0.05 µmol **NiP**, 2.25 mL electron donor solution (0.1 M AA, pH 4.5), AM 1.5 G,100 mW cm^{-2}, λ > 420 nm, 25 °C.

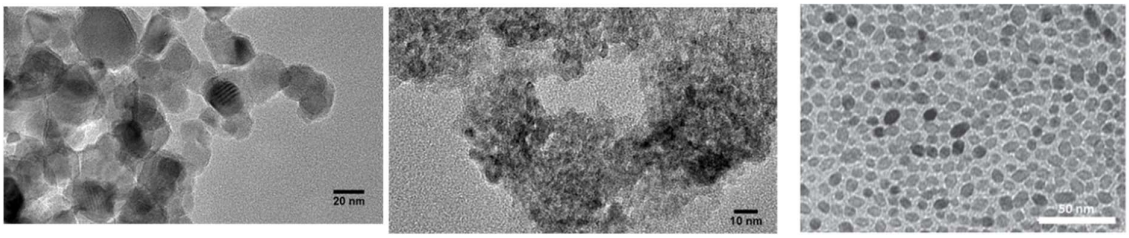

Figure S8. Left to right: TEM of P25, AN10, and AN7-TiO_2 nanoparticles.

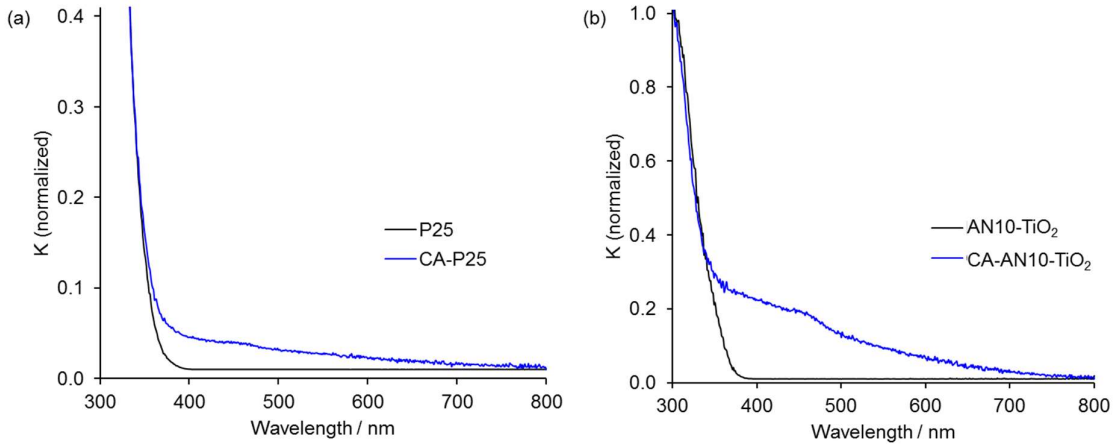

Figure S9. Diffuse reflectance spectra of (a) CA-P25 and (b) CA-AN10-TiO_2 nanoparticles (1 wt% in Ba_2SO_4). Spectra are normalised to the absorption at 300 nm.

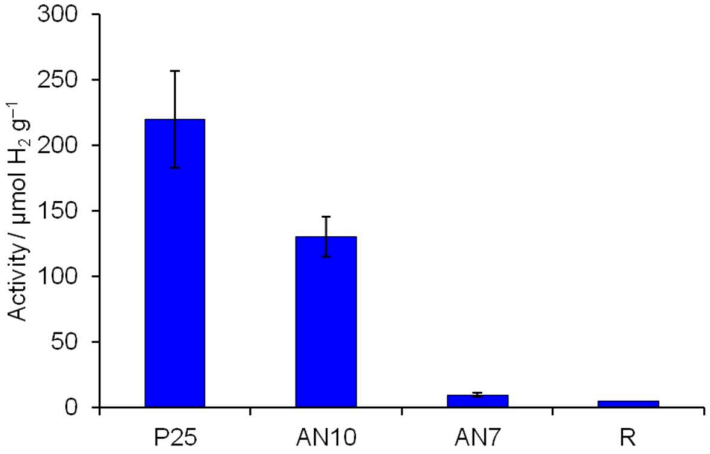

Figure S10. Effect of particle type on H_2 evolution activity after 3 h for caffeic acid (CA)-functionalised TiO_2 nanoparticles. Conditions: 2.5 mg powder, 0.05 µmol **NiP**, 2.25 mL electron donor solution (0.1 M AA, pH 4.5), AM 1.5 G, 100 mW cm^{-2}, λ > 420 nm, 25 °C. AN10 = commercial anatase, 10 nm; AN7 = in-house synthesised anatase, 7 nm; R = commercial rutile, 10 – 30 nm.

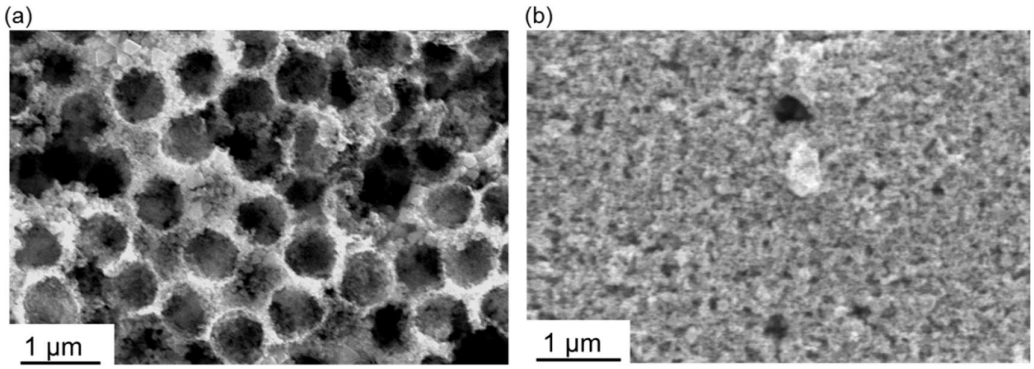

Figure S11. SEM of (a) IO-ITO and (b) mesoITO.

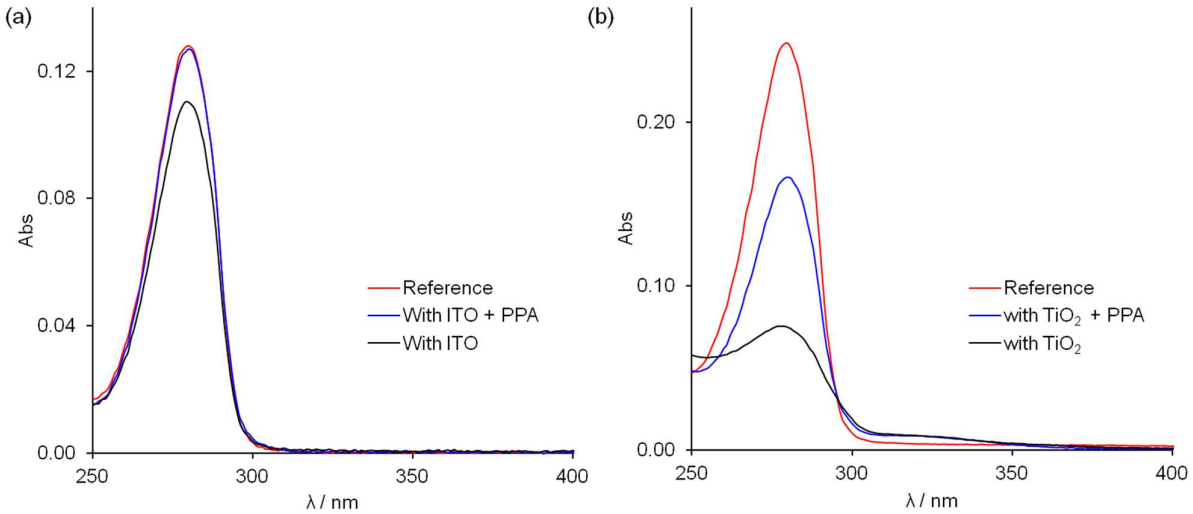

Figure S12. UV-vis spectroscopy of an aqueous DHCA solution before (Reference curve, red) and after exposure to (a) IO-ITO electrodes and (b) P25 TiO_2 powder, in the presence (blue curve) or absence (black curve) of 1 equivalent of propylphosphonic acid (PPA).

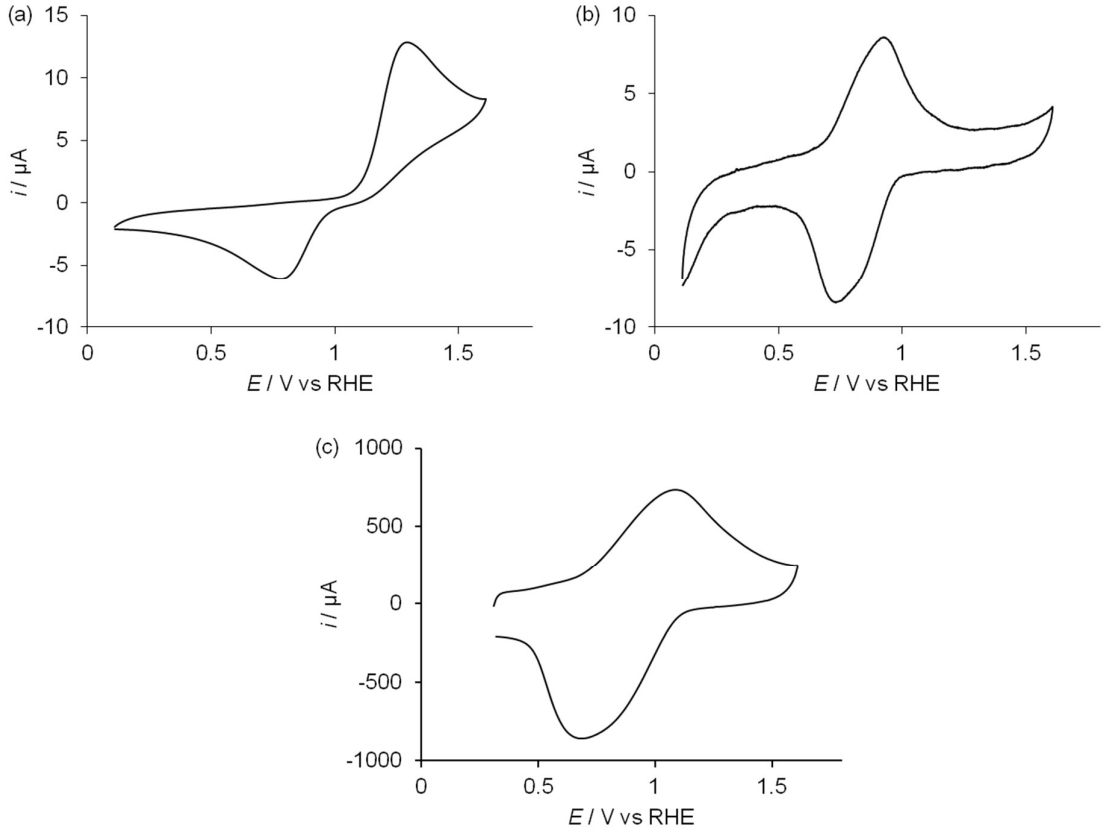

Figure S13. Cyclic voltammetry (50 mV s^{-1}, room temperature) of DHSP (a) in solution (1 mM, 0.1 M phosphate buffer, pH 7, glassy carbon working electrode) and immobilised on (b) flat ITO and (c) IO-ITO (0.1 M Na_2SO_4, pH 7). Immobilisation improves the reversibility of the redox couple and shifts $E_{1/2}$ by ~200 mV (1.03 V for (a) and 0.84 V for (b)).

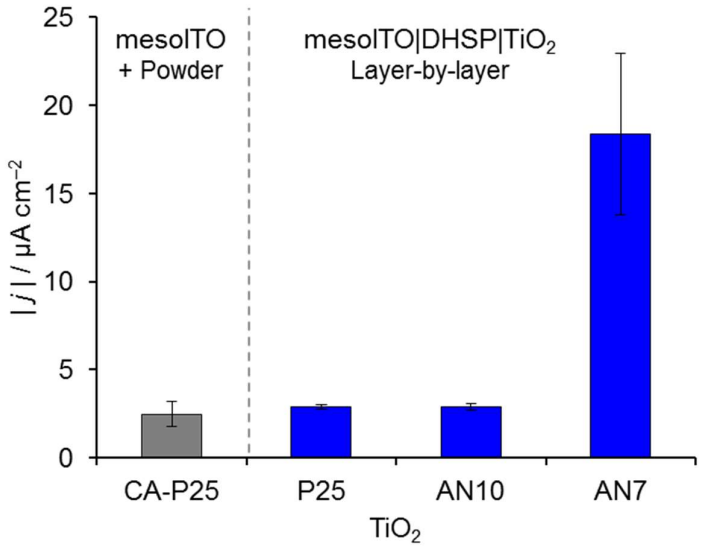

Figure S14. Comparison of the magnitude of photocurrent obtained in chronoamperometry under air (O_2 as electron acceptor) with TiO_2 deposited onto mesoITO electrodes (0.1 M Na_2SO_4, pH 4.5, 0.3 V *vs.* RHE, room temperature, λ > 400 nm, 100 mW cm^{-2}). Irradiation of mesoITO and mesoITO|DHSP alone (no TiO_2) did not generate photocurrent (see also Fig. 3a).

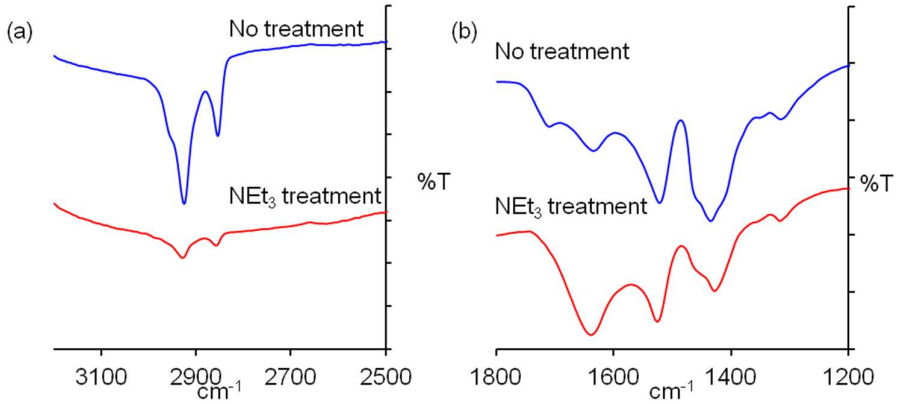

Figure S15. FT-IR of flat ITO|DHSP|AN7-TiO_2 before and after treatment with NEt_3. After treatment, the C-H (a) and COOH (b) stretching frequencies are reduced in amplitude.

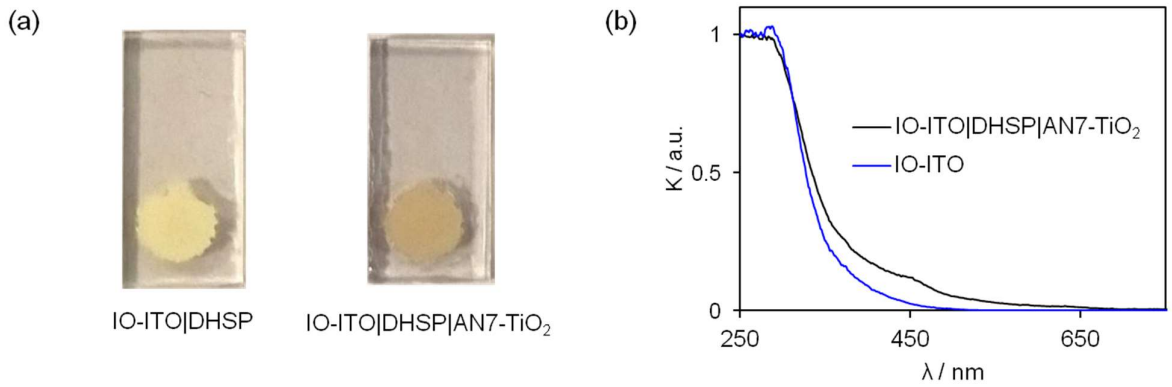

Figure S16. (a) Photographs and (b) normalised diffuse reflectance UV-vis absorption spectra of IO-ITO electrodes showing colouration upon immobilisation of TiO_2 due to formation of the charge-transfer interactions. Active electrode area = 0.25 cm^2.

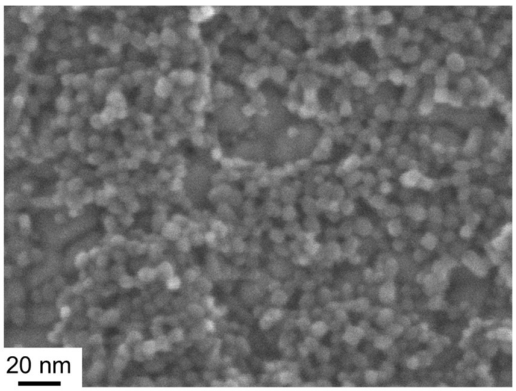

Figure S17. High resolution SEM of an AN7-TiO_2 nanoparticle film on flat ITO|DHSP.

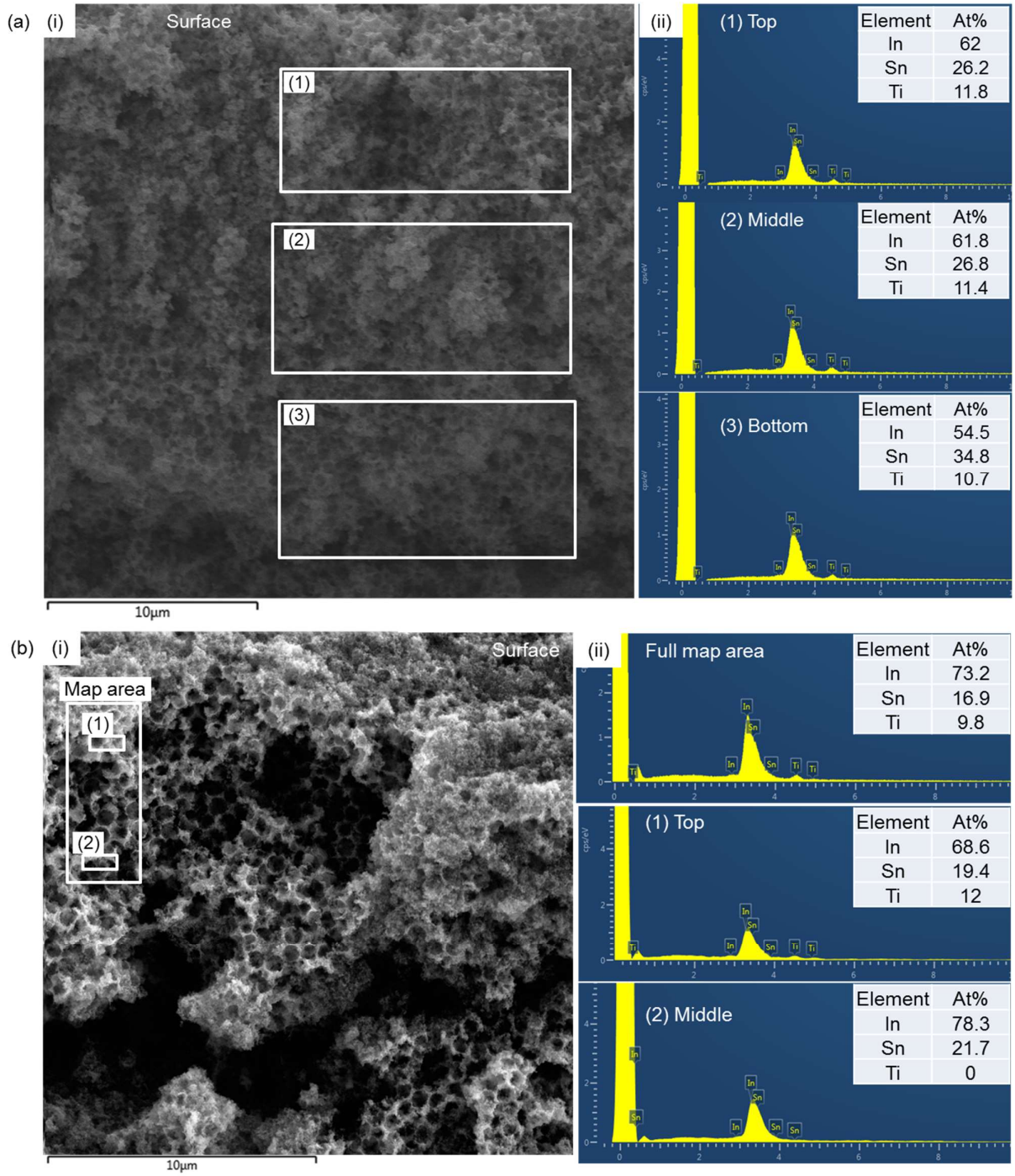

Figure S18. EDX analysis of IO-ITO|DHSP|TiO_2 electrodes (i) cross-sectional SEM image showing analysis regions and (ii) EDX spectra and analysis data for (a) AN7-TiO_2 and (b) P25 TiO_2.

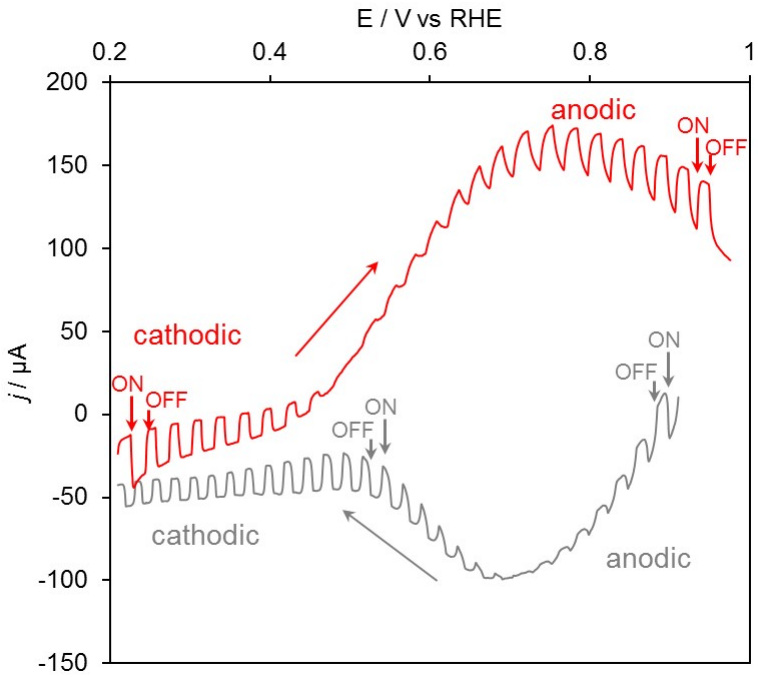

Figure S19. Dependence of the photocurrent response of IO-ITO|DHSP|AN7-TiO_2 under air on applied potential (0.1 M Na_2SO_4, pH 7). Arrows indicate direction of the scan and where the light was turned on or off (100 mW cm^{-2}, λ > 400 nm, room temperature).

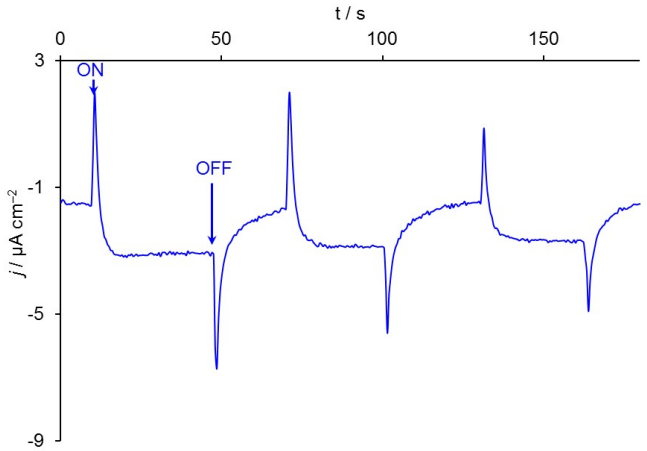

Figure S20. Chronoamperometry at 0.3 V *vs*. RHE of IO-ITO|DHSP|AN7-TiO_2 under N_2 atmosphere (0.1 M Na_2SO_4, pH 4.5, 100 mW cm^{-2}, λ > 400 nm, room temperature).

Supporting References

1. M. A. Gross, A. Reynal, J. R. Durrant and E. Reisner, *J. Am. Chem. Soc.*, 2014, **136**, 356-366.
2. H. Krawczyk and Ł. Albrecht, *Synthesis*, 2005, **2005**, 2887-2896.
3. M. Kato, T. Cardona, A. W. Rutherford and E. Reisner, *J. Am. Chem. Soc.*, 2013, **135**, 10610-10613.
4. D. Mersch, C.-Y. Lee, J. Z. Zhang, K. Brinkert, J. C. Fontecilla-Camps, A. W. Rutherford and E. Reisner, *J. Am. Chem. Soc.*, 2015, **137**, 8541-8549.
5. C.-Y. Lee, B. Reuillard, K. P. Sokol, T. Laftsoglou, C. W. J. Lockwood, S. F. Rowe, E. T. Hwang, J. C. Fontecilla-Camps, L. J. C. Jeuken, J. N. Butt and E. Reisner, *Chem. Commun.*, 2016, **52**, 7390-7393.
6. I. A. Mudunkotuwa, T. R. Anthony, V. H. Grassian and T. M. Peters, *J. Occup. Environ. Hyg.*, 2016, **13**, 30-39.
7. W.-L. Wang, S. C. Chai, M. Huang, H.-Z. He, T. D. Hurley and Q.-Z. Ye, *J. Med. Chem.*, 2008, **51**, 6110-6120.
8. E. T. Hwang, K. Sheikh, K. L. Orchard, D. Hojo, V. Radu, C.-Y. Lee, E. Ainsworth, C. Lockwood, M. A. Gross, T. Adschiri, E. Reisner, J. N. Butt and L. J. C. Jeuken, *Adv. Funct. Mater.*, 2015, **25**, 2308-2315.
9. G. Zhang and W. Choi, *Chem. Commun.*, 2012, **48**, 10621-10623.
10. E. L. Rosen, R. Buonsanti, A. Llordes, A. M. Sawvel, D. J. Milliron and B. A. Helms, *Angew. Chem. Int. Ed.*, 2012, **51**, 684-689.
11. Y. Ooyama, M. Kanda, K. Uenaka and J. Ohshita, *ChemPhysChem*, 2015, **16**, 3049-3057.
12. Y. Xu and M. A. A. Schoonen, *Am. Mineral.*, 2000, **85**, 543-556.

End of Electronic Supporting Information